

Supplementary Material

Imagen analysis

The evolution of the microstructure was visualized with the acquisition of multiple images, in the beginning, at the end of each shear period, and when the flow stopped completely. The images were spaced at intervals of 1 s for statistical analysis, as shown in Figure S1.

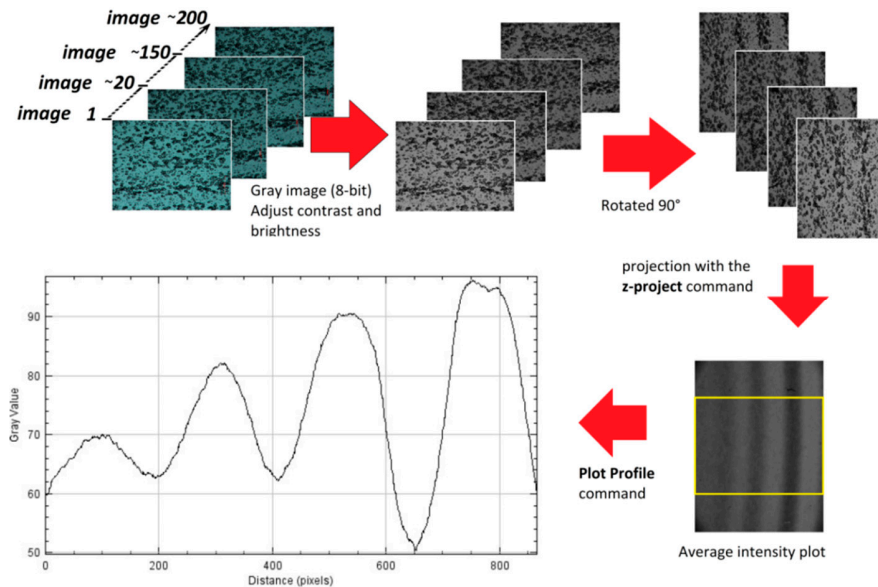


Figure S1. Scheme of the image analysis procedure for the description of the evolution of band formation. It is essential to include the flow direction with an arrow. The stacking of images correspond to the $\dot{\gamma} = 4.5 \text{ s}^{-1}$.

To extract the information from the captured images, we proceed in steps. These steps are: (a) The capture: this stage is the experimental arrangement, the camera, the zoom. (b) The pre-processing: where the noise of images is reduced, and those details that are not of interest in the experiment are eliminated. (c) The segmentation: here, the drops to be measured are evaluated according to size and shape criteria. The extraction of the characteristics: here, we proceed to obtain the chosen measurements of each of the objects, images, and stacks.

The observation of bands in the direction of vorticity is analyzed quantitatively using ImageJ® software and compared systematically against changes due to increments in the applied shear rate. The stage of pre-processing, segmentation, and extraction of the images are shown in Figure S1. The ~200 images captured during the flow are collected for each shear, i.e., six collections of approximately 200 images each. These ~200 images are stacked and rotated 90° in an anti-clockwise direction to favor the analysis and subsequent visualization of the results. Subsequently, the stack is converted to 8-bit grayscale, also adjusting the contrast and brightness of the stack.

Later, a projection with the z-project command is made — remember that the z-project command analyzes stacks by applying six different methods of projection of pixels of the stack. The six techniques of the z-project command are shown in Figure S2, where each of the images is the result of applying the z-project command to the same shear rate (of 4.5 s^{-1}) image. In Figure S2, all six techniques are presented. Each technique allows us to visualize the formation of bands in a unique way; for example, in some cases, the band is shown in black and others in white or is not visible.

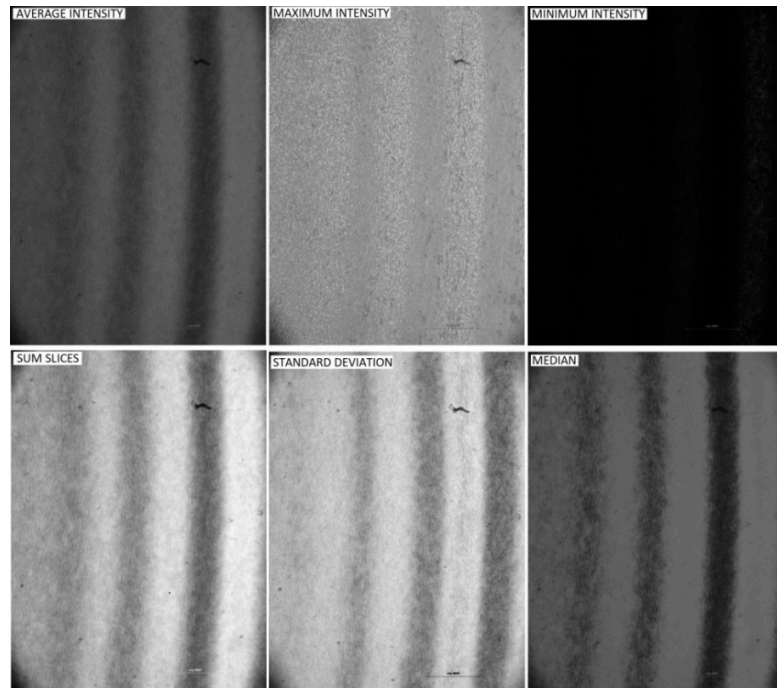


Figure S2. The z-project techniques for banding analysis. From left to right: average intensity, maximum intensity, minimum intensity, sum slices, standard deviation, and median.

To choose the most favorable technique for our purposes. Each technique was graphed of intensity vs. radial distance of the whole image is made with the plot profile function, as can be seen in Figure S3. The graph obtained of intensity vs. radial distance shows undulations, where intervals of intensity — where zero is equal to black and 255 to white — are used.

For example, when using Average, minimum sum, and median graphs, valleys represent areas (regions) with the highest droplet population during flow, and crests, vice versa. Conversely, the same happens with the techniques of maximum intensity and standard deviation.

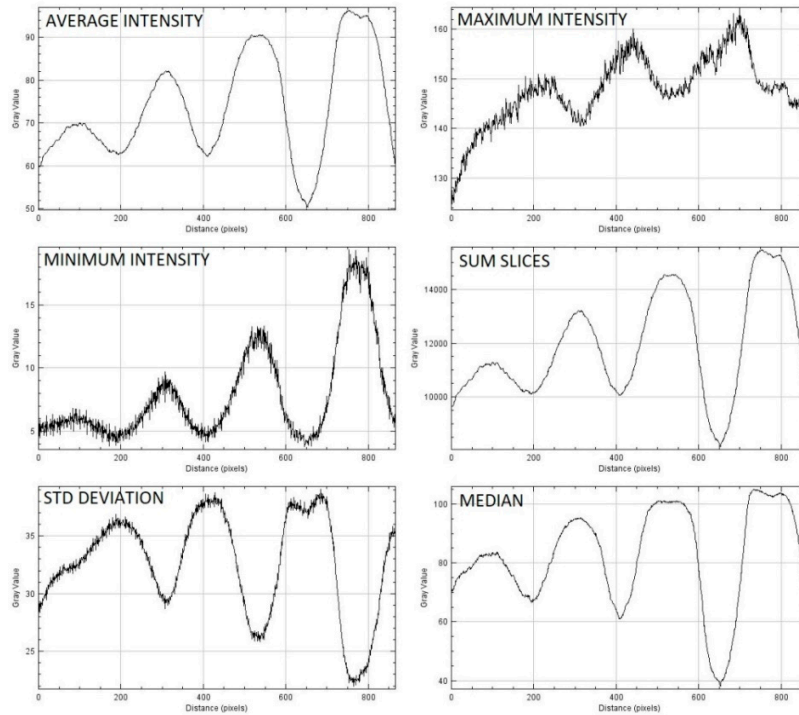


Figure S3. The plot of the intensity vs. radial distance graph of z-project techniques for banding analysis. From left to right: average intensity, maximum intensity, minimum intensity, sum slices, standard deviation, and median.

For example, when using Average, minimum sum, and median graphs, valleys represent areas (regions) with the highest droplet population during flow, and crests, vice versa. Conversely, the same happens with the techniques of maximum intensity and standard deviation.

Thus, the average intensity technique is chosen here for the analysis, for it provides be the most accurate method for our purposes. The noise is minimal and allows identifying the evolution of the population of droplets at the borders of the bands. To facilitate understanding of the data, the gray hue of the average intensity technique is inverted.

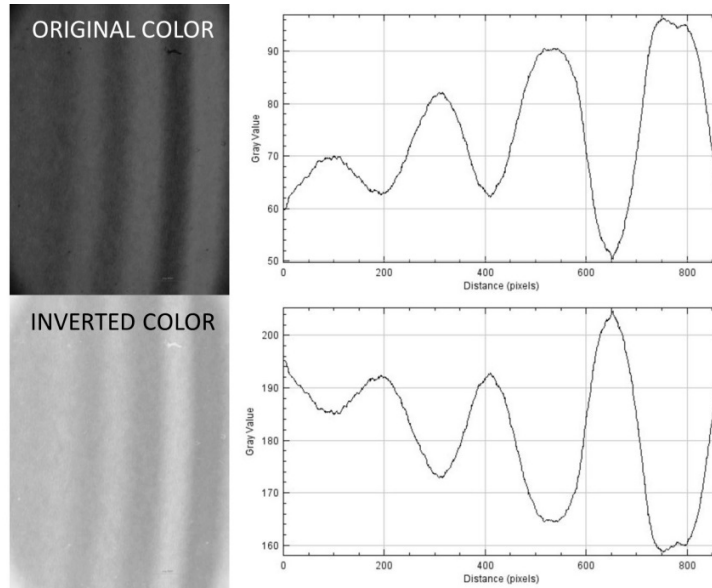


Figure S4. Image obtained with the average intensity technique with color inversion (left side) and its graph of intensity vs. radial distance (px) for a $\dot{\gamma} = 4.5 \text{ s}^{-1}$ (right plots). In the image of inverted colors, valleys correspond to a low population of drops and peaks to a high population of drops.

In this manner, at the moment of making intensity vs. radial distance graphs, each valley represents the low population of drops, and each peak the high population of drops, as shown in Figure S4. Hence, the projection on the perpendicular axis of the image plane is made with the average intensity technique for each single shear rate.

The described methodology is applied to each of the studied shear rates, as shown in Figure S5.; the abscissa corresponds to the position along the vorticity axis, while the ordinate contains data of the normalized intensities [0, 1]. Image processing provides information on the average position of the peak of the band at all times of the evolution. As well, it is possible to make a qualitative comparison of the number of drops in each zone by evaluating the *relative* height of each peak (with regard to the intensity of the valley). Figure S5 shows the profiles obtained from stacking images for various shear rates. Only shear rates higher than 3.0 s^{-1} the show, clearly, band formation.

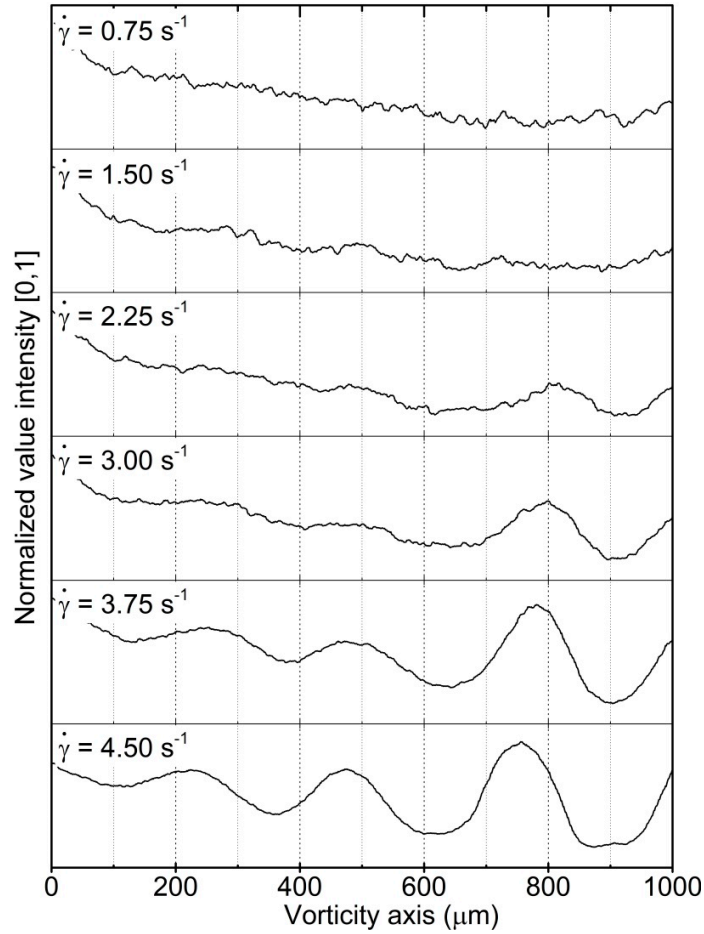


Figure S5. Intensity vs. radial distance graph from 0.75 to 4.5 s^{-1} , each 0.75 (top to bottom). Formation and displacement of the bands. The intensity axis was normalized from 0 to 1.

In order to determine the long-time evolution of each band, a second statistical analysis is carried out. The objective is to characterize the intensity data by adjusting a Gaussian curve with parameters shown in Figure S6. The amplitude (A), the Full Width at Half Maximum (FWHM), and the position of the peak (X_c) are the parameters taken into account for the acquisition of the width of the band, the population of the drops, and the possible displacement of the peak.

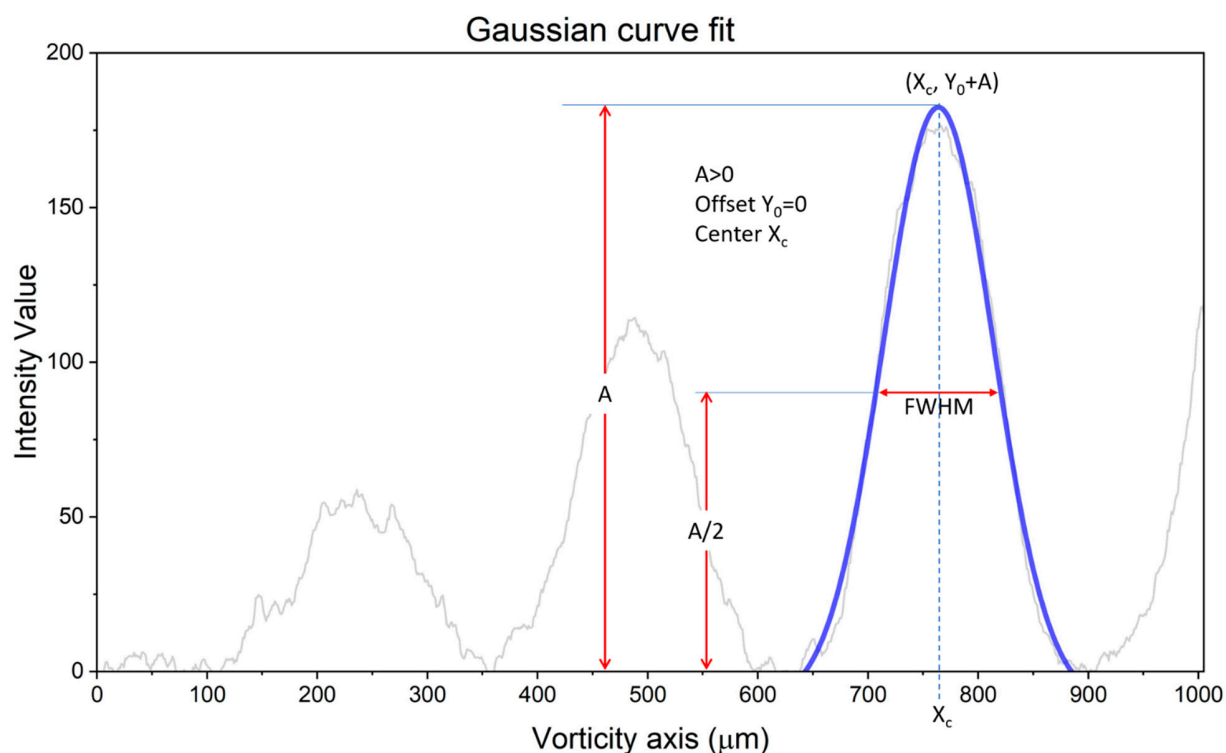


Figure S6. Plot the average intensity of 10 images (1 fps) for a $\dot{\gamma} = 4.5 \text{ s}^{-1}$. The parameters obtained from the adjustment of a Gaussian curve are indicated.

Figure S7 shows the four parameters that characterized the dynamics of each peak. Each intensity vs. position plot is composed of 867 columns (aligned with the flow direction), and each column has 1155 intensity values. Thus, each plot of the graph — plots Figure S7b and 8d — represents the mean value of the intensity for 11,550 readings produced with ten images at a specific time in the drops distribution evolution.

The black trace in Figure S7a corresponds to the mean intensity value for that column. Intense (and light) red bands show the uncertainty range at each column, indicating that large fluctuations are due to a large number of drops passing by. However, as is shown in Figure S5, fitting a Gaussian curve to peaks on intensity plots requires setting a common baseline at both ends of the curve, i.e., traces shown in Figure S7c and S7e.

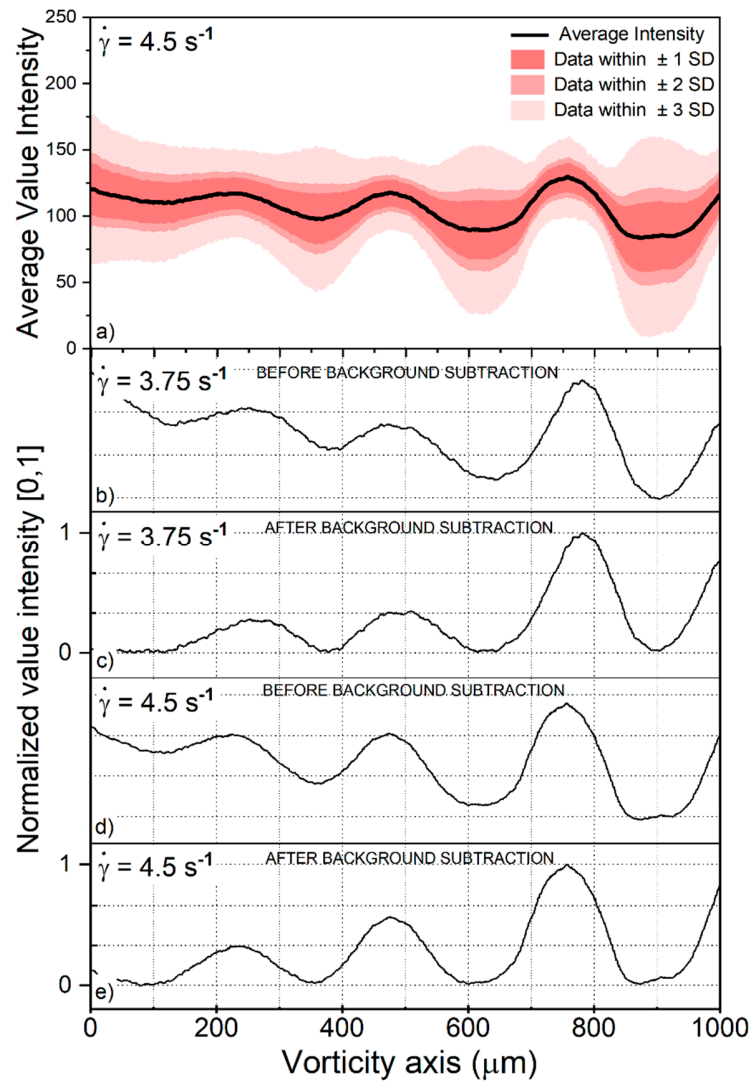


Figure S7. Intensity vs. vorticity axis (μm) of a pack of 10 images (1 fps) for $\dot{\gamma} = 3.0 \text{ s}^{-1}$ and 4.5 s^{-1} . Plot (a) shows the black trace for the mean intensity at each column, while red bands correspond to their uncertainties. Plots (b) and (d) correspond to raw intensities, while (c) and (e) to intensities with a baseline correction.

Thus, Figure S8 shows the adjustment carried out for the two highest shear rates.

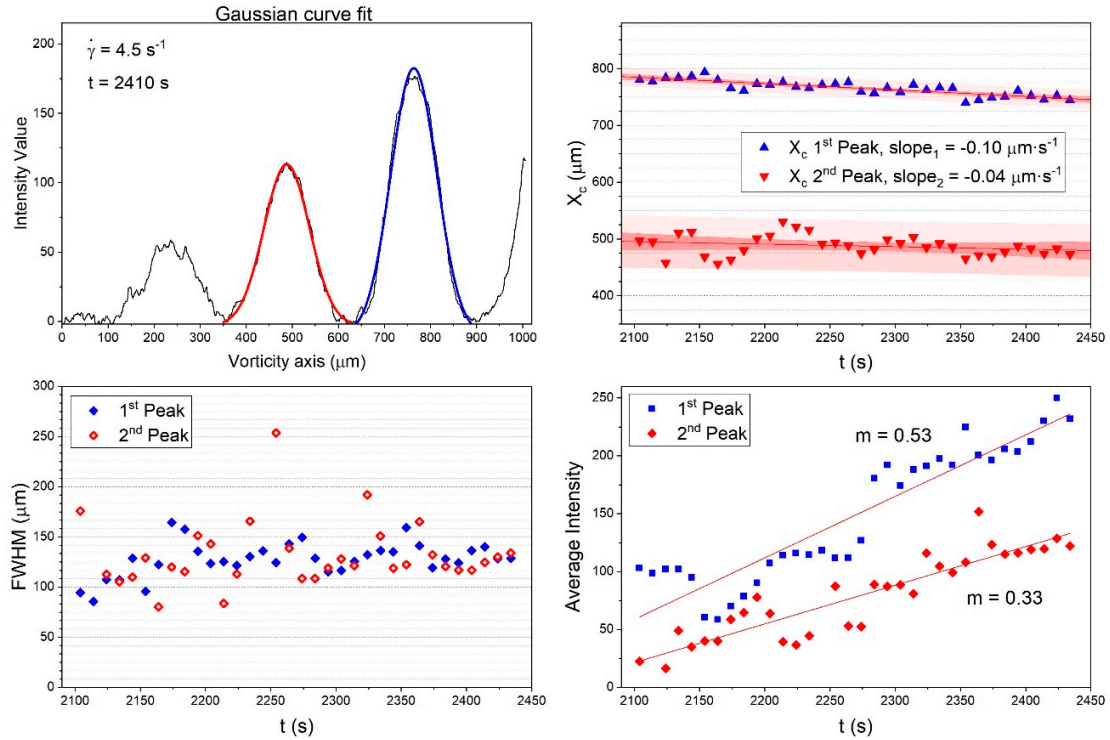


Figure S8. On the left upper side is the graph of intensity vs. vorticity axis (μm) of a pack of 10 images (1 fps) for an applied $\dot{\gamma} = 4.5 \text{ s}^{-1}$. The mean time of $t=2410 \text{ s}$ corresponds to the elapsed time from the start of the experiment to the capture of the image packet. The top and right graph corresponds to the peak position displacement observed for all 34 ministacks, i.e., x_c vs. time for the two most significant peaks. On the lower side are the graph of FWHM and of intensity vs. time, respectively. Blue data points correspond to the rightmost peak and red point to the middle peak.

For the analysis shown in Figure S8, the plots are the average intensity (vs. position along the vorticity axis) with an adjusted baseline. The *time tag* for this data set corresponds to ten images, around 2410 s, after the onset of flow at 5 s^{-1} . These images were corresponding to 10 s of flow, with a total time of 337 images for the entire stack. Thus, the information is coalesced into thirty-four mini-stacks (34 data points) to track the complete time evolution of the peak dynamics, i.e., duration of the experiment.

The blue and red solid traces (Figure S8a) are the adjusted Gaussian curves that best describes the intensities of those bands. Properties for the Gaussian trace indicate that its FWHM width remains roughly constant at $135 \mu\text{m}$ after 2150 s of flow for both bands. In contrast, the growing amplitude indicates that the number of drops on the band is still increasing, but at a rate proportional to its height. The trace of x_{ci} vs. *time* measures the leftward displacement of the peak beginning at 2000 s after the onset of flow. The mean lateral displacement velocity of the peak is higher for the right peak at $-\text{slope}_1 = 0.10 \mu\text{m}\cdot\text{s}^{-1}$ (toward the center of rotation of the flow cell).

The measurement of the velocity of the banded (peaks) and non-banded (valleys) zones for the $\dot{\gamma} = 4.5 \text{ s}^{-1}$ was performed manually. Table S1 shows the number of droplets used to determine the velocity and to obtain the average velocity shown in Figure 3.

Table S1. Data on the number of drops observed to determine the average band (and non-band) velocity for the $\dot{\gamma} = 4.5 \text{ s}^{-1}$.

| | N | Median value position vorticity axis | Mean velocity | Standard Deviation |
|-----------------------------|----|--|------------------|-----------------------|
| <i>valley still forming</i> | 26 | 90.60 | 192.02 | 6.21 |
| <i>peak still forming</i> | 41 | 259.00 | 196.28 | 12.33 |
| Valley | 27 | 398.84 | 203.24 | 10.18 |
| Peak | 32 | 564.96 | 198.00 | 11.73 |
| Valley | 17 | 703.00 | 199.68 | 7.36 |
| Peak | 34 | 855.46 | 199.08 | 12.90 |
| Valley | 21 | 992.99 | 208.76 | 12.44 |